Detailed fluctuation theorem from the one-time measurement scheme

Kenji Maeda [,1] Tharon Holdsworth [,1] Sebastian Deffner [,2] and Akira Sone [1,*]

[1]*Department of Physics, University of Massachusetts, Boston, Massachusetts 02125, USA*
[2]*Department of Physics, University of Maryland, Baltimore County, Baltimore, Maryland 21250, USA*

We study the quantum fluctuation theorem in the one-time measurement (OTM) scheme, where the work distribution of the backward process has been lacking and which is considered to be more informative than the two-time measurement (TTM) scheme. We find that the OTM scheme is the quantum nondemolition TTM scheme, in which the final state is a pointer state of the second measurement whose Hamiltonian is conditioned on the first measurement outcome. Then, by clarifying the backward work distribution in the OTM scheme, we derive the detailed fluctuation theorem in the OTM scheme for the characteristic functions of the forward and backward work distributions, which captures the detailed information about the irreversibility and can be applied to quantum thermometry. We also verified our conceptual findings with the IBM quantum computer. Our result clarifies that the laws of thermodynamics at the nanoscale are dependent on the choice of the measurement and may provide experimentalists with a concrete strategy to explore laws of thermodynamics at the nanoscale by protecting quantum coherence and correlations.

Introduction. One of the most significant conceptual factors distinguishing quantum physics and classical physics is *measurement* [1]. In quantum mechanics, measurements typically destroy quantum coherences and correlations that could be utilized as the resources for many quantum engineering tasks, such as quantum computing and quantum metrology. Compared to classical systems, one has many degrees of freedom in choosing the basis of the measurement based on their task on the quantum system. Particularly, the eigenbasis of the observable of the measurement apparatus is comprised of the so-called pointer states [2–6], which are immune to decoherence due to the corresponding measurement.

Quantum thermodynamics [7–9] is a rapidly growing field exploring the laws of thermodynamics from the perspective of quantum information science. Fluctuation theorems [10,11] in both quantum and classical systems are regarded as one of the most significant laws to date [12] because many significant thermodynamic principles can be derived, such as the second law of thermodynamics [13] and response theory [14,15]. The standard approach toward quantum fluctuation theorem is the so-called two-time measurement (TTM) scheme [16–31].

The TTM scheme is constructed by two energy projection measurements at the beginning and the end of a quantum process. In the standard setup of the time-varying Hamiltonian system, the initial state is prepared in the Gibbs state defined by its initial Hamiltonian H_0. Then, one performs an energy measurement on the initial state with H_0, which projects the system onto one of the eigenstates $|E_i\rangle$ of H_0 based on the initial measurement outcome E_i. Then, one evolves the system under the unitary operator U during time τ and measures the evolved state $U|E_i\rangle$ with the final Hamiltonian H_τ. Finally, the

system will be projected again onto an eigenstate $|E_j'\rangle$ of H_τ based on the final measurement outcome E_j'.

The work performed on the system in a single realization is defined by the difference between the final and initial measurement outcome, $W_{i\rightarrow j} \equiv E_j' - E_i$, which recovers the standard fluctuation theorem, also known as the TTM fluctuation theorem resembling the classical Jarzynksi equality [10]. Therefore, the TTM scheme can be regarded as a *semiclassical* approach, which has been experimentally implemented in various systems [32–42], including a demonstration on the DWave machine [30]. However, the second projection measurement usually destroys the quantum coherence and correlations generated through the dynamics, which means that the TTM cannot fully capture the peculiar features of the quantum systems when one analyzes its thermodynamic behaviors [29].

To address the thermodynamic contribution of quantum correlations, Ref. [43] proposed the so-called one-time measurement (OTM) scheme. In this scheme, the second measurement is considered to be avoided and the work is determined by the energy difference conditioned on the initial energy measurement outcome. Within this paradigm, the corresponding Jarzynski equality includes the additional information contribution stemming from the quantum relative entropy of the conditional thermal state [44,45] with respect to the Gibbs state defined by the final Hamiltonian. This additional term provides a tighter maximum work relation and captures the quantum coherence or correlations generated through the dynamics in the formalism. Therefore, the OTM scheme can be regarded as more informative than the TTM scheme. This has been elucidated in various contexts, including quantum thermometry [45], work as an external quantum observable [46], distinguishability of heat and work in an open quantum system [47], heat exchange [48], classical correspondence of the OTM scheme [44], quantum ergotropy

_____
*akira.sone@umb.edu

[49], and information production [50]. However, the backward process in the OTM scheme has not been considered yet, which has made the detailed quantum fluctuation theorem of the OTM scheme elusive.

In the present Letter, we first prove that the OTM scheme is the quantum nondemolition (QND) TTM scheme, where the pointer states of the second measurement (conditional Hamiltonian) are the evolved states conditioned on the initial measurement outcome. From this, we construct the backward work distribution and derive the detailed quantum fluctuation theorem of the OTM scheme, which we call *OTM fluctuation theorem*. Then, we propose a quantum circuit to compute the symmetric relation of the characteristic functions of the forward and backward work distributions. We explore the physical meaning of the OTM fluctuation theorem by associating it to the concept of irreversibility and demonstrate the potential application of the derived formalism to state preparation for low-temperature quantum thermometry. Finally, we verify the derived detailed fluctuation theorem with IBM quantum computer to demonstrate the experimental implementability of the OTM scheme. These results emphasize that the laws of quantum thermodynamics are strictly determined by the choice of measurements by the observers.

OTM detailed fluctuation theorem. Our first result is the derivation of the OTM fluctuation theorem. We consider a finite-dimensional closed quantum system described by a d-dimensional Hilbert space. Let the initial state be a Gibbs state $\rho_0^{\mathrm{eq}} \equiv \exp(-\beta H_0)/Z_0$, where H_0 is the initial Hamiltonian and $Z_0 \equiv \mathrm{tr}\{\exp(-\beta H_0)\}$ is the partition function. In a closed quantum system, the time evolution is described by a unitary operator U. In the OTM scheme, the work for a single realization of the protocol is defined as

$$\widetilde{W}_i \equiv \langle E_i | U^\dagger H_\tau U | E_i \rangle - E_i, \quad (1)$$

which also has been called *conditional work* [44]. This is the energy difference between the final energy conditioned on the initial measurement outcome and itself. Then, the forward conditional work distribution is simply given by [43]

$$\widetilde{P}_f(W) = \sum_{i=1}^d \frac{e^{-\beta E_i}}{Z_0} \delta(W - \widetilde{W}_i), \quad (2)$$

which is consistent with the exact average work

$$\langle W \rangle = \int W \widetilde{P}_f(W) dW = \mathrm{tr}\{(U^\dagger H_\tau U - H_0)\rho_0^{\mathrm{eq}}\} \quad (3)$$

and yields the generalized Jarzynski equality [43]

$$\langle e^{-\beta W} \rangle_{\widetilde{P}} = \frac{\widetilde{Z}_\tau}{Z_0} = e^{-\beta \Delta F} e^{-S(\widetilde{\rho}_\tau || \rho_\tau^{\mathrm{eq}})}. \quad (4)$$

In Eq. (4), the conditional partition function, $\widetilde{Z}_\tau \equiv \sum_{i=1}^d \exp(-\beta \langle E_i | U^\dagger H_\tau U | E_i \rangle)$, is the normalization factor used to construct the conditional thermal state,

$$\widetilde{\rho}_\tau \equiv \sum_{i=1}^d \frac{e^{-\beta \langle E_i | U^\dagger H_\tau U | E_i \rangle}}{\widetilde{Z}_\tau} U | E_i \rangle \langle E_i | U^\dagger. \quad (5)$$

Finally, $S(\widetilde{\rho}_\tau || \rho_\tau^{\mathrm{eq}}) = \mathrm{tr}\{\widetilde{\rho}_\tau \ln \widetilde{\rho}_\tau\} - \mathrm{tr}\{\widetilde{\rho}_\tau \ln \rho_\tau^{\mathrm{eq}}\}$ is the quantum relative entropy of the conditional thermal state with

respect to the Gibbs state $\rho_\tau^{\mathrm{eq}} \equiv \exp(-\beta H_\tau)/Z_\tau$ of the final Hamiltonian H_τ.

By comparing with the TTM scheme, we demonstrate that the OTM scheme is equivalent to the TTM scheme with a carefully chosen final Hamiltonian (conditional Hamiltonian) based on the information about the initial measurement outcome and the dynamics of the system. To see this point, let us define the conditional Hamiltonian G_τ,

$$G_\tau \equiv \sum_{i=1}^d \langle E_i | U^\dagger H_\tau U | E_i \rangle U | E_i \rangle \langle E_i | U^\dagger, \quad (6)$$

where E_i is the eigenenergy of the initial Hamiltonian H_0 with its corresponding eigenstate $|E_i\rangle$. At $t = 0$ we perform a projective energy measurement H_0 on the system initially prepared in ρ_0^{eq}. Then, the postmeasurement state will be projected onto $|E_i\rangle$ with the corresponding energy E_i. After the evolution, the state is $U|E_i\rangle$. At $t = \tau$ we perform the second measurement G_τ. Since the final state is a *pointer state* of G_τ, it is not destroyed by the measurement, so that the observer obtains the final energy measurement outcome $\langle E_i | U^\dagger H_\tau U | E_i \rangle$, while the system remains as $U|E_i\rangle$. The corresponding quantum work is simply given by Eq. (1).

Then, the equivalent work distribution within the TTM paradigm, the forward work distribution is computed as

$$\widetilde{P}_f(W) = \sum_{i=1}^d \frac{e^{-\beta \langle E_i | H_0 | E_i \rangle}}{Z_0} |\langle E_i | U^\dagger U | E_i \rangle|^2 \delta(W - \widetilde{W}_i), \quad (7)$$

which is identical to Eq. (2).

This is our *first main result*, namely we have that the OTM scheme is exactly the QND TTM scheme, in which the second projection measurement does not destroy the evolved state conditioned on the initial measurement outcome (see Fig. 1 and [51]). We will now exploit this insight to construct the conditional work distribution for the backward process within the OTM paradigm.

The backward process is initialized from the state $\widetilde{\rho}_\tau \equiv \exp(-\beta G_\tau)/\widetilde{Z}_\tau$. After the backward evolution described by $U^\dagger$, the measurement H_0 is performed on the final state of the backward process. Since the final state is $U^\dagger U | E_i \rangle = | E_i \rangle$, which is a pointer state of H_0, H_0 does not destroy the state. Moreover, the outcome is always E_i.

Then, by following the TTM scheme, the conditional work distribution of the backward process is given by

$$\widetilde{P}_b(-W) \equiv \sum_{i=1}^d \frac{e^{-\beta \langle E_i | U^\dagger H_\tau U | E_i \rangle}}{\widetilde{Z}_\tau} \delta(-W + \widetilde{W}_i). \quad (8)$$

From Eq. (8) we now derive the fluctuation theorem [52–54] between the forward conditional work distribution and backward distribution in the characteristic function form.

The characteristic functions are defined as the Fourier transform of the work distributions

$$\widetilde{C}_f(u) \equiv \int dW \, \widetilde{P}_f(W) e^{iuW},$$

$$\widetilde{C}_b(u) \equiv \int dW \, \widetilde{P}_b(-W) e^{-iuW}. \quad (9)$$
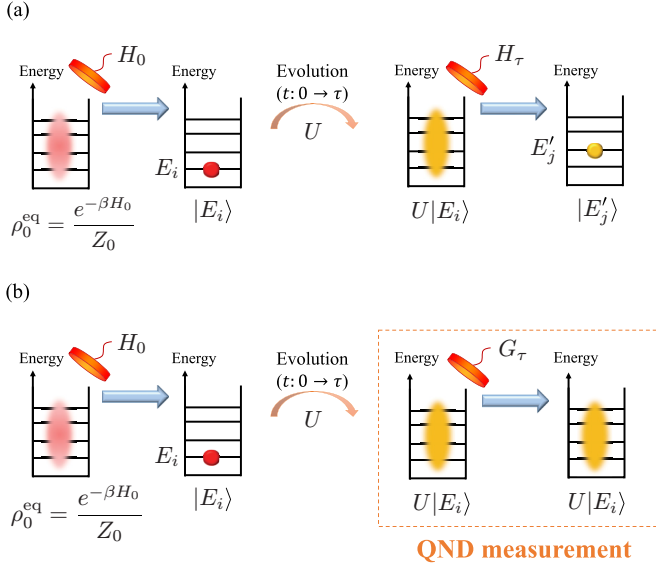
(a)

(b)

QND measurement

FIG. 1. Comparison between the TTM and OTM scheme. In (a) the standard TTM scheme, in which the second energy measurement is the final Hamiltonian, the projection measurement projects the evolved state $U|E_i\rangle$ onto $|E_j'\rangle$ the eigenstate of H_τ. In (b) the OTM scheme, the final Hamiltonian $G_\tau \equiv \sum_{i=1}^{d}\langle E_i|U^\dagger H_\tau U|E_i\rangle U|E_i\rangle\langle E_i|U^\dagger$ is the conditional Hamiltonian with its pointer state $U|E_i\rangle$, which is equivalent to the evolved state conditioned on the initial measurement outcome. Therefore, this measurement preserves the state $U|E_i\rangle$. In this sense, this measurement is a QND measurement.

By applying the approach to the TTM scheme in Refs. [52–54], the characteristic functions are equivalent to

$$\widetilde{C}_f(u) = \mathrm{tr}\{U^\dagger e^{iuG_\tau} U\, e^{-iuH_0}\rho_0^{\mathrm{eq}}\},$$
$$\widetilde{C}_b(u) = \mathrm{tr}\{U\, e^{iuH_0} U^\dagger e^{-iuG_\tau}\widetilde{\rho}_\tau\}. \qquad (10)$$

Thus we obtain the following symmetry relation [55], which is our *second main result*:

$$\frac{\widetilde{C}_f(u)}{\widetilde{C}_b(-u+i\beta)} = \frac{\widetilde{Z}_\tau}{Z_0} = e^{-\beta\Delta F - S(\widetilde{\rho}_\tau||\rho_\tau^{\mathrm{eq}})}, \qquad (11)$$

where

$$\widetilde{C}_b(-u+i\beta) = \mathrm{tr}\{U\, e^{-iuH_0} e^{-\beta H_0} U^\dagger e^{iuG_\tau} e^{\beta G_\tau}\widetilde{\rho}_\tau\}. \qquad (12)$$

The characteristic functions can be determined directly from quantum circuits, and hence our results permit the demonstration of the experimental implementability of the OTM scheme in the single qubit interferometry.

Single-qubit interferometry approach. By employing the single-qubit interferometry approach developed in Refs. [53,54], we now construct a quantum algorithm to verify Eq. (11). This indicates that the OTM scheme is experimentally implementable, which is our *third main result*.

Let us define $|0\rangle \equiv (1\;\;\;0)^T$ and $|1\rangle \equiv (0\;\;\;1)^T$. We denote by $\mathbb{1}$ the 2×2 identity matrix and X, Y, Z as the usual Pauli matrices. Also, we write the Hadamard gate as $\mathbf{H} \equiv \frac{1}{\sqrt{2}}\binom{1\;\;\;1}{1\;\;-1}$. Then, the characteristic function of the forward process $\widetilde{C}_f(u)$ can be computed by the quantum circuit depicted in Fig. 2. In this circuit, the ancilla qubit is initially prepared in $|0\rangle$. The target system is prepared in the
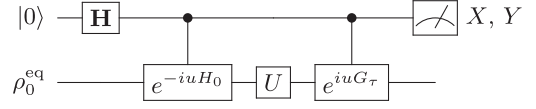

FIG. 2. Quantum circuit for computing $\widetilde{C}_f(u)$. The expectation values of X and Y obtained by measuring the final state of the ancilla qubit are $\mathrm{Re}[\widetilde{C}_f(u)]$ and $\mathrm{Im}[\widetilde{C}_f(u)]$, respectively.

Gibbs state ρ_0^{eq}. To obtain the characteristic function $\widetilde{C}_f(u)$, we measure the output state of the ancilla qubit with X and Y, whose expectation values become $\langle X\rangle = \mathrm{Re}[\widetilde{C}_f(u)]$ and $\langle Y\rangle = \mathrm{Im}[\widetilde{C}_f(u)]$.

Next, we consider the quantum circuit to compute the characteristic function of the backward process $\widetilde{C}_b(-u+i\beta)$. From Eq. (12), we need to first decompose $\exp(\beta G_\tau)$ and $\exp(-\beta H_0)$ with Pauli string $\{\sigma_k\}_{k=1}^{d^2}$, where σ_1 is the $d\times d$ identity matrix [56]. Here, note that $\frac{1}{d}\mathrm{tr}\{\sigma_k\sigma_\ell\} = \delta_{k\ell}$ becomes Kronecker's delta. Then, we can write $\exp(-\beta H_0) = \sum_{k=1}^{d^2}\alpha_k^{(0)}\sigma_k$ and $\exp(\beta G_\tau) = \sum_{k=1}^{d^2}\alpha_k^{(\tau)}\sigma_k$, where $\alpha_k^{(0)} = \frac{1}{d}\mathrm{tr}\{e^{-\beta H_0}\sigma_k\}$ and $\alpha_k^{(\tau)} = \frac{1}{d}\mathrm{tr}\{e^{\beta G_\tau}\sigma_k\}$. Note that the coefficients $\{\alpha_k^{(0)}, \alpha_k^{(\tau)}\}_{k=1}^{d^2}$ are computable via a classical computer since we have full knowledge of H_0, H_τ, and U if d is smaller. Therefore, we can write

$$\widetilde{C}_b(-u+i\beta) = \sum_{k,\ell}\alpha_k^{(0)}\alpha_\ell^{(\tau)}F_{k\ell}, \qquad (13)$$

where we define

$$F_{k\ell} \equiv \mathrm{tr}\{U\sigma_k e^{-iuH_0} U^\dagger \sigma_\ell e^{iuG_\tau}\widetilde{\rho}_\tau\}. \qquad (14)$$

Then, we can employ the quantum circuit depicted in Fig. 3 to compute $F_{k\ell}$. In this circuit, the ancilla qubit is prepared in $|0\rangle$. The target system is prepared in the conditional thermal state $\widetilde{\rho}_\tau$. Here, the expectation values become $\langle X\rangle = \mathrm{Re}[F_{k\ell}]$ and $\langle Y\rangle = \mathrm{Im}[F_{k\ell}]$. Given the fact that we have already known $\{\alpha_k^{(0)}, \alpha_k^{(\tau)}\}_{k=1}^{d^2}$ via a classical computer, from Eq. (13), we can finally obtain $\widetilde{C}_b(-u+i\beta)$.

Physical meaning of OTM fluctuation theorem. By considering the backward process, we can find that the OTM fluctuation theorem can capture the detailed information about the irreversibility and be applied to state preparation for quantum thermometry in the low-temperature limit. To quantify the irreversibility of a quantum process, we consider the Kullback-Leibler (KL) divergence $D[\widetilde{P}_f||\widetilde{P}_b]$ of $\widetilde{P}_f(W)$ with respect to $\widetilde{P}_b(-W)$, which is defined as

$$D[\widetilde{P}_f||\widetilde{P}_b] \equiv \int dW\, \widetilde{P}_f(W)\ln\left(\frac{\widetilde{P}_f(W)}{\widetilde{P}_b(-W)}\right). \qquad (15)$$

From Eqs. (2) and (8), we obtain [51]

$$D[\widetilde{P}_f||\widetilde{P}_b] = -S(\rho_0^{\mathrm{eq}}) + \beta\,\mathrm{tr}\{U\rho_0^{\mathrm{eq}}U^\dagger H_\tau\} + \ln\widetilde{Z}_\tau, \qquad (16)$$
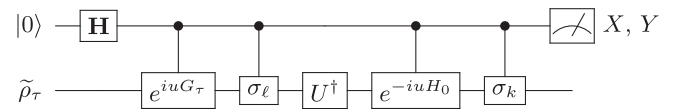

FIG. 3. Quantum circuit for computing $F_{k\ell}$. The expectation values of X and Y obtained by measuring the final state of the ancilla qubit are $\mathrm{Re}[F_{k\ell}]$ and $\mathrm{Im}[F_{k\ell}]$, respectively.

where $S(\rho_0^{\mathrm{eq}}) \equiv -\mathrm{tr}\{\rho_0^{\mathrm{eq}} \ln \rho_0^{\mathrm{eq}}\}$ is the von Neumann entropy of ρ_0^{eq}. Given that the exact averaged work $\langle W \rangle \equiv \mathrm{tr}\{U\rho_0^{\mathrm{eq}}U^\dagger H_\tau\} - \mathrm{tr}\{\rho_0^{\mathrm{eq}} H_0\}$, from Eq. (11), the excess work $\langle W_{\mathrm{ex}} \rangle \equiv \langle W \rangle - \Delta F$ can be written as

$$\beta \langle W_{\mathrm{ex}} \rangle = D[\widetilde{P}_f || \widetilde{P}_b] + S(\widetilde{\rho}_\tau || \rho_\tau^{\mathrm{eq}}). \tag{17}$$

This means that the excess work $\langle W_{\mathrm{ex}} \rangle$ is a sum of the KL divergence $D[\widetilde{P}_f || \widetilde{P}_b]$, which characterizes the irreversible process, and $\beta S(\widetilde{\rho}_\tau || \rho_\tau^{\mathrm{eq}})$, which is the energy dissipated into the heat bath when the system is thermalized from $\widetilde{\rho}_\tau$. Therefore, $\beta S(\widetilde{\rho}_\tau || \rho_\tau^{\mathrm{eq}})$ can be interpreted as a heatlike quantity.

Furthermore, $D[\widetilde{P}_f || \widetilde{P}_b]$ can be employed in quantum thermometry in the low-temperature limit. In Ref. [45], it was demonstrated that the conditional thermal state $\widetilde{\rho}_\tau$ can outperform the Gibbs state ρ_τ^{eq} in the low-temperature limit. Therefore, preparing $\widetilde{\rho}_\tau$ is a desired task for quantum thermometry. First the excess work can be written as $\beta \langle W_{\mathrm{ex}} \rangle = S(U\rho_0^{\mathrm{eq}}U^\dagger || \rho_\tau^{\mathrm{eq}})$ [57–59]. In Ref. [45], we derived the so-called thermodynamic triangle equality $S(U\rho_0^{\mathrm{eq}}U^\dagger || \widetilde{\rho}_\tau) + S(\widetilde{\rho}_\tau || \rho_\tau^{\mathrm{eq}}) = S(U\rho_0^{\mathrm{eq}}U^\dagger || \rho_\tau^{\mathrm{eq}})$. Therefore, from Eq. (17), we obtain

$$D[\widetilde{P}_f || \widetilde{P}_b] = S(U\rho_0^{\mathrm{eq}}U^\dagger || \widetilde{\rho}_\tau), \tag{18}$$

which measures the distinguishability of the exact final state $U\rho_0^{\mathrm{eq}}U^\dagger$ and the conditional thermal state $\widetilde{\rho}_\tau$. This quantity can be used to design the unitary process U that minimizes $S(U\rho_0^{\mathrm{eq}}U^\dagger || \widetilde{\rho}_\tau)$ for the final exact state $U\rho_0^{\mathrm{eq}}U^\dagger$ to be closer to $\widetilde{\rho}_\tau$. Also, note that the distinguishability measure $S(U\rho_0^{\mathrm{eq}}U^\dagger || \widetilde{\rho}_\tau)$ can be computed by a quantum computer. From Eqs. (11) and (16), we have

$$D[\widetilde{P}_f || \widetilde{P}_b] = \beta \langle W \rangle + \ln \left(\frac{\widetilde{C}_f(u)}{\widetilde{C}_b(-u + i\beta)} \right), \tag{19}$$

where $\langle W \rangle$, $\widetilde{C}_f(u)$, and $\widetilde{C}_b(-u + i\beta)$ can be computed by a quantum computer.

Finally, we emphasize that these analyses are hard to conduct within the TTM scheme [31]. Therefore, our detailed fluctuation demonstrates an additional advantage of the OTM scheme.

Verification with IBM quantum computers. To conclude our analysis, we employ the IBM cloud-based quantum computer [60] to verify the detailed fluctuation theorem (11). Our setup is the following. The initial Hamiltonian H_0 is $H_0 = \omega(Z \otimes \mathbb{1} + \mathbb{1} \otimes Z)$ with the corresponding eigenbasis $|E_1\rangle = (1 \quad 0 \quad 0 \quad 0)^T$, $|E_2\rangle = (0 \quad 1 \quad 0 \quad 0)^T$, $|E_3\rangle = (0 \quad 0 \quad 1 \quad 0)^T$, and $|E_4\rangle = (0 \quad 0 \quad 0 \quad 1)^T$. The final Hamiltonian is set to be $H_\tau = J(X \otimes X)$. The unitary operator that describes the evolution is set as $U = \exp[-i\frac{\Omega\tau}{2}(Y \otimes \mathbb{1} + \mathbb{1} \otimes Y)]$.

For the initial Gibbs state preparation, we consider the decomposition of the input mixed state. This is because we can only prepare pure states on the IBM quantum computers and $\{|E_i\rangle\}_{i=1}^4$ can be prepared. For the weights $\{\exp(-\beta E_i)/Z_0\}_{i=1}^4$,
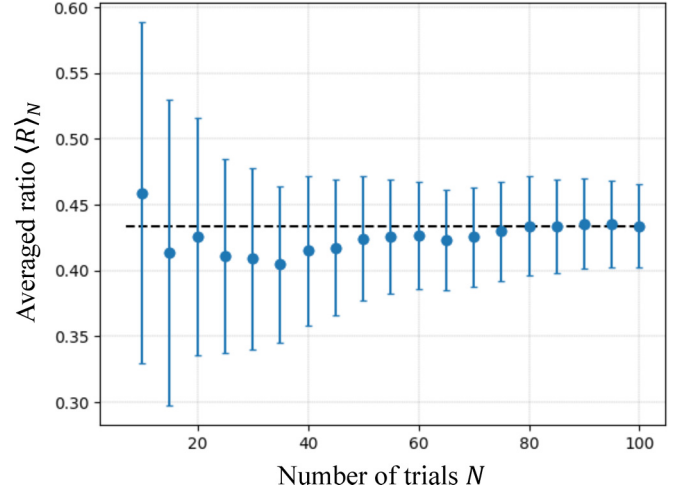

FIG. 4. Verification with IBM quantum computers. The dashed line is the exact value $R_{\mathrm{true}} = 0.433167$. The error bars represent 99% confidence interval. As we increase the number of trials N, the averaged ratios $\langle R \rangle_N$ approach the exact value with a clear plateau starting from $N = 75$. When $N = 100$, we have $\langle R \rangle_{100} = 0.433706$.

since we already know the initial Hamiltonian H_0, we assume that the weights are also known and we can compute $\widetilde{C}_f(u)$.

For the backward process, we need to prepare the conditional thermal state $\widetilde{\rho}_\tau$ as the initial state. In our simulation, we suppose that we already know U; therefore, we can prepare $\{U|E_i\rangle\}_{i=1}^4$ with the quantum computer. Similarly, because we assume that U, H_0, and H_τ are known, the weights $\{\exp(-\beta \langle E_i | U^\dagger H_\tau U | E_i\rangle)/\widetilde{Z}_\tau\}_{i=1}^4$ are considered to be also known, which we use to compute $F_{k\ell}$. Thus the coefficients $\alpha_k^{(0)}$ and $\alpha_\ell^{(\tau)}$ are also regarded as known values, which enables one to compute $\widetilde{C}_b(-u + i\beta)$.

By setting the parameters as $\beta = 0.5$, $\omega = 2$, $\Omega = 3$, $J = 1$, and $\tau = \pi/4$, we obtain the theoretical value of the ratio

$$R_{\mathrm{true}} \equiv \frac{\widetilde{C}_f(u)}{\widetilde{C}_b(-u + i\beta)} = 0.433167 \tag{20}$$

for any u. Here, we particularly focus on the case $u = 1$ and verify Eq. (20) with the IBM cloud-based quantum computer [60].

To determine $\langle X \rangle$ and $\langle Y \rangle$, for each quantum circuit in Figs. 2 and 3, we perform the single-shot measurement 20000 times. The median of the errors of the gates and the single-qubit readout error in our setup are around 10^{-4}–10^{-2} with the T_1 and T_2 ranging from around 17 μs to 232 μs (for complete information of the IBM machine, refer to the Supplemental Material [51]). Because of the error, the computed ratio becomes complex; therefore, we consider the absolute value of the ratio $R \equiv |\widetilde{C}_f(1)/\widetilde{C}_b(-1 + 0.5i)|$. To obtain more precise values, we run the whole process N times (number of trials) and compare the true value with the average value $\langle R \rangle_N \equiv \frac{1}{N} \sum_{j=1}^N R_j$, where R_j is the value of R at the jth trial. Then, we compute the error rate as $e_N = |1 - \langle R \rangle_N / R_{\mathrm{true}}| \times 100 \, [\%]$ for each N.

We have achieved a very high accuracy in our simulation. In Fig. 4, we plot the relation between $\langle R \rangle_N$ for each number of trials $N = 10, 15, 20, \ldots, 100$, where the error bars represent the 99% confidence interval [61]. As we can see, as
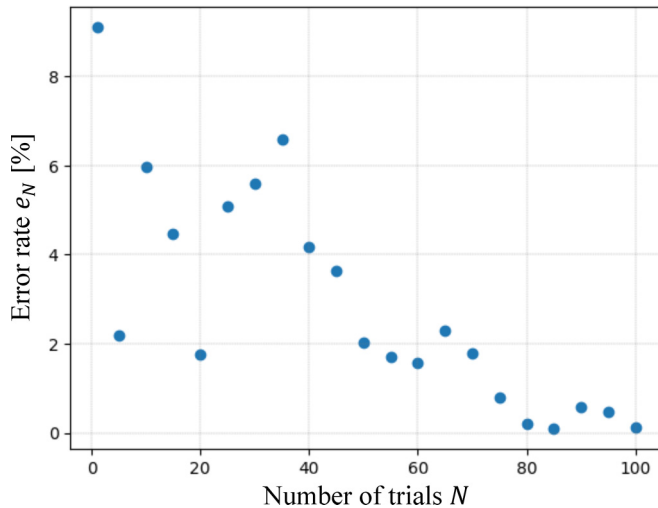
FIG. 5. Error rate vs number of trials. As we increase the number of trials N, the error rate e_N becomes smaller. When $N = 100$, we have $e_{100} \simeq 0.12\%$.

we increase the number of trials, the average value converges to the true value with an explicit plateau starting from $N = 75$. When $N = 100$, $\langle R \rangle_{100}$ records 0.433706.

In Fig. 5, we show the relation between the error rate e_N and the number of trials N. As we can see, as the number of trials increases, the error rate becomes smaller. Actually, when $N = 100$, e_{100} records around 0.12%, which is accurate

enough to claim that the OTM fluctuation theorem Eq. (11) is verified with the IBM quantum computer.

Conclusion. In conclusion, we have derived the detailed fluctuation theorem of the OTM scheme by clarifying the backward work distribution. This has been enabled by the insight that the OTM scheme can be regarded as a QND TTM scheme, where the second measurement is constructed by the pointer states conditioned on the initial energy measurement outcome. We have related its physical meaning to the irreversibility and quantum thermometry in the low-temperature limit. We have also demonstrated its experimental implementability and we have verified the derived fluctuation theorem on the IBM quantum computer by introducing the corresponding quantum circuit to compute the symmetric relation between the characteristic functions of the forward and backward work distributions. These results not only provide the solutions to the open problems regarding the OTM scheme, but also clarify that the laws of thermodynamics at the nanoscale are strictly dependent on the choice of the measurement of the observer. From a practical point of view, these results provide experimentalists with a concrete strategy to study laws of thermodynamics at the nanoscale by protecting quantum coherence and correlations.

[1] M. A. Nielsen and I. L. Chuang, *Quantum Computation and Quantum Information: 10th Anniversary Edition*, 10th ed. (Cambridge University Press, New York, 2010).

[2] W. H. Zurek, Pointer basis of quantum apparatus: Into what mixture does the wave packet collapse? Phys. Rev. D **24**, 1516 (1981).

[3] M. A. Schlosshauer, *Decoherence: and the Quantum-to-Classical Transition* (Springer Science & Business Media, New York, 2007).

[4] C. A. Brasil and L. A. de Castro, Understanding the pointer states, Eur. J. Phys. **36**, 065024 (2015).

[5] A. Touil, B. Yan, D. Girolami, S. Deffner, and W. H. Zurek, Eavesdropping on the decohering environment: Quantum Darwinism, amplification, and the origin of objective classical reality, Phys. Rev. Lett. **128**, 010401 (2022).

[6] W. H. Zurek, Decoherence, einselection, and the quantum origins of the classical, Rev. Mod. Phys. **75**, 715 (2003).

[7] S. Deffner and S. Campbell, *Quantum Thermodynamics* (Morgan and Claypool Publishers, San Rafael, 2019).

[8] S. Vinjanampathy and J. Anders, Quantum thermodynamics, Contemp. Phys. **57**, 545 (2016).

[9] F. Binder, L. A. Correa, C. Gogolin, J. Anders, and G. Adesso, *Thermodynamics in the Quantum Regime* (Springer, Berlin, 2019).

[10] C. Jarzynski, Nonequilibrium equality for free energy differences, Phys. Rev. Lett. **78**, 2690 (1997).

[11] G. E. Crooks, Entropy production fluctuation theorem and the nonequilibrium work relation for free energy differences, Phys. Rev. E **60**, 2721 (1999).

[12] J. M. O. de Zárate, Interview with Michael E. Fisher, Europhys. News **42**, 14 (2011).

[13] C. Jarzynski, Equalities and inequalities: Irreversibility and the second law of thermodynamics at the nanoscale, Annu. Rev. Condens. Matter Phys. **2**, 329 (2011).

[14] D. Andrieux and P. Gaspard, Quantum work relations and response theory, Phys. Rev. Lett. **100**, 230404 (2008).

[15] D. Andrieux, P. Gaspard, T. Monnai, and S. Tasaki, The fluctuation theorem for currents in open quantum systems, New J. Phys. **11**, 043014 (2009).

[16] H. Tasaki, Jarzynski relations for quantum systems and some applications, arXiv:cond-mat/0009244.

[17] J. Kurchan, A quantum fluctuation theorem, arXiv:cond-mat/0007360.

[18] P. Talkner, E. Lutz, and P. Hänggi, Fluctuation theorems: Work is not an observable, Phys. Rev. E **75**, 050102(R) (2007).

[19] C. Jarzynski and D. K. Wójcik, Classical and quantum fluctuation theorems for heat exchange, Phys. Rev. Lett. **92**, 230602 (2004).

[20] Y. Morikuni, H. Tajima, and N. Hatano, Quantum Jarzynski equality of measurement-based work extraction, Phys. Rev. E **95**, 032147 (2017).

[21] A. E. Rastegin, Non-equilibrium equalities with unital quantum channels, J. Stat. Mech. (2013) P06016.

[22] C. Jarzynski, H. T. Quan, and S. Rahav, Quantum-classical correspondence principle for work distributions, Phys. Rev. X **5**, 031038 (2015).

[23] L. Zhu, Z. Gong, B. Wu, and H. T. Quan, Quantum-classical correspondence principle for work distributions in a chaotic system, Phys. Rev. E **93**, 062108 (2016).

[24] R. Pan, Z. Fei, T. Qiu, J.-N. Zhang, and H. T. Quan, Quantum-classical correspondence of work distributions for initial states with quantum coherence, arXiv:1904.05378.

[25] D. Kafri and S. Deffner, Holevo's bound from a general quantum fluctuation theorem, Phys. Rev. A **86**, 044302 (2012).

[26] J. Goold, M. Paternostro, and K. Modi, Nonequilibrium quantum Landauer principle, Phys. Rev. Lett. **114**, 060602 (2015).

[27] A. E. Rastegin and K. Życzkowski, Jarzynski equality for quantum stochastic maps, Phys. Rev. E **89**, 012127 (2014).

[28] J. Goold and K. Modi, Fluctuation theorem for nonunital dynamics, AVS Quantum Sci. **3**, 045001 (2021).

[29] M. Perarnau-Llobet, E. Bäumer, K. V. Hovhannisyan, M. Huber, and A. Acin, No-go theorem for the characterization of work fluctuations in coherent quantum systems, Phys. Rev. Lett. **118**, 070601 (2017).

[30] B. Gardas and S. Deffner, Quantum fluctuation theorem for error diagnostics in quantum annealers, Sci. Rep. **8**, 17191 (2018).

[31] A. Kiely, E. O'Connor, T. Fogarty, G. T. Landi, and S. Campbell, Entropy of the quantum work distribution, Phys. Rev. Res. **5**, L022010 (2023).

[32] G. Huber, F. Schmidt-Kaler, S. Deffner, and E. Lutz, Employing trapped cold ions to verify the quantum Jarzynski equality, Phys. Rev. Lett. **101**, 070403 (2008).

[33] A. Smith, Y. Lu, S. An, X. Zhang, J.-N. Zhang, Z. Gong, H. T. Quan, C. Jarzynski, and K. Kim, Verification of the quantum nonequilibrium work relation in the presence of decoherence, New J. Phys. **20**, 013008 (2018).

[34] S. An, J.-N. Zhang, M. Um, D. Lv, Y. Lu, J. Zhang, Z.-Q. Yin, H. T. Quan, and K. Kim, Experimental test of the quantum Jarzynski equality with a trapped-ion system, Nat. Phys. **11**, 193 (2015).

[35] T. B. Batalhão, A. M. Souza, L. Mazzola, R. Auccaise, R. S. Sarthour, I. S. Oliveira, J. Goold, G. De Chiara, M. Paternostro, and R. M. Serra, Experimental reconstruction of work distribution and study of fluctuation relations in a closed quantum system, Phys. Rev. Lett. **113**, 140601 (2014).

[36] S. Hernández-Gómez, S. Gherardini, F. Poggiali, F. S. Cataliotti, A. Trombettoni, P. Cappellaro, and N. Fabbri, Experimental test of exchange fluctuation relations in an open quantum system, Phys. Rev. Res. **2**, 023327 (2020).

[37] S. Hernández-Gómez, N. Staudenmaier, M. Campisi, and N. Fabbri, Experimental test of fluctuation relations for driven open quantum systems with an NV center, New J. Phys. **23**, 065004 (2021).

[38] D. Collin, F. Ritort, C. Jarzynski, S. B. Smith, I. Tinoco, and C. Bustamante, Verification of the Crooks fluctuation theorem and recovery of RNA folding free energies, Nature (London) **437**, 231 (2005).

[39] J. M. R. Parrondo, J. M. Horowitz, and T. Sagawa, Thermodynamics of information, Nat. Phys. **11**, 131 (2015).

[40] S. Toyabe, T. Sagawa, M. Ueda, E. Muneyuki, and M. Sano, Experimental demonstration of information-to-energy conversion and validation of the generalized Jarzynski equality, Nat. Phys. **6**, 988 (2010).

[41] Z. Zhang, T. Wang, L. Xiang, Z. Jia, P. Duan, W. Cai, Z. Zhan, Z. Zong, J. Wu, L. Sun, Y. Yin, and G. Guo, Experimental demonstration of work fluctuations along a shortcut to adiabaticity with a superconducting xmon qubit, New J. Phys. **20**, 085001 (2018).

[42] D. Hahn, M. Dupont, M. Schmitt, D. J. Luitz, and M. Bukov, Quantum many-body Jarzynski equality and dissipative noise on a Digital Quantum computer, Phys. Rev. X **13**, 041023 (2023).

[43] S. Deffner, J. P. Paz, and W. H. Zurek, Quantum work and the thermodynamic cost of quantum measurements, Phys. Rev. E **94**, 010103(R) (2016).

[44] A. Sone and S. Deffner, Jarzynski equality for stochastic conditional work, J. Stat. Phys. **183**, 11 (2021).

[45] A. Sone, D. Soares-Pinto, and S. Deffner, Conditional quantum thermometry–enhancing precision by measuring less, arXiv:2304.13595.

[46] K. Beyer, K. Luoma, and W. T. Strunz, Work as an external quantum observable and an operational quantum work fluctuation theorem, Phys. Rev. Res. **2**, 033508 (2020).

[47] A. Sone, Y.-X. Liu, and P. Cappellaro, Quantum Jarzynski equality in open quantum systems from the one-time measurement scheme, Phys. Rev. Lett. **125**, 060602 (2020).

[48] A. Sone, D. O. Soares-Pinto, and S. Deffner, Exchange fluctuation theorems for strongly interacting quantum pumps, AVS Quantum Sci. **5**, 032001 (2023).

[49] A. Sone and S. Deffner, Quantum and classical ergotropy from relative entropies, Entropy **23**, 1107 (2021).

[50] A. Sone, N. Yamamoto, T. Holdsworth, and P. Narang, Jarzynski-like equality of nonequilibrium information production based on quantum cross entropy, Phys. Rev. Res. **5**, 023039 (2023).

[51] See Supplemental Material at http://link.aps.org/supplemental/10.1103/PhysRevA.108.L050203 for (1) the explanation of why the OTM scheme is a QND TTM scheme, (2) the derivation of the detailed fluctuation theorem and the symmetric relation for the general case that the initial state is also the conditional thermal state, (3) the derivation of the KL divergence $D[\widetilde{P}_f||\widetilde{P}_b]$, (4) the details of the experimental verification of the symmetric relation in the two-qubit case, and (5) the detailed information about the IBM machines that we used.

[52] M. Campisi, P. Hänggi, and P. Talkner, Colloquium: Quantum fluctuation relations: Foundations and applications, Rev. Mod. Phys. **83**, 771 (2011).

[53] L. Mazzola, G. De Chiara, and M. Paternostro, Measuring the characteristic function of the work distribution, Phys. Rev. Lett. **110**, 230602 (2013).

[54] R. Dorner, S. R. Clark, L. Heaney, R. Fazio, J. Goold, and V. Vedral, Extracting quantum work statistics and fluctuation theorems by single-qubit interferometry, Phys. Rev. Lett. **110**, 230601 (2013).

[55] In the Supplemental Material [51], we provide the proof for the case that the initial state is also the conditional thermal state

defined by $G_0 \equiv \sum_{i=1}^{d} \langle \psi_i | H_0 | \psi_i \rangle | \psi_i \rangle \langle \psi_i |$, with $| \psi_i \rangle$ being not necessarily the eigenstate of H_0. Equation (11) can be regarded as its corollary.

[56] When $d = 4$, the Pauli string is $\{\mathbb{1}, X \otimes \mathbb{1}, Y \otimes \mathbb{1}, Z \otimes \mathbb{1}, \mathbb{1} \otimes X, \mathbb{1} \otimes Y, \mathbb{1} \otimes Z, X \otimes X, X \otimes Y, X \otimes Z, Y \otimes X, Y \otimes Y, Y \otimes Z, Z \otimes X, Z \otimes Y, Z \otimes Z\}$, which has $4^2 = 16$ elements, and these elements are the bases constructing any 4×4 matrix.

[57] S. Deffner and E. Lutz, Generalized Clausius inequality for nonequilibrium quantum processes, Phys. Rev. Lett. **105**, 170402 (2010).

[58] R. Kawai, J. M. R. Parrondo, and C. Van den Broeck, Dissipation: The phase-space perspective, Phys. Rev. Lett. **98**, 080602 (2007).

[59] S. Vaikuntanathan and C. Jarzynski, Dissipation and lag in irreversible processes, Europhys. Lett. **87**, 60005 (2009).

[60] A. Cross, The IBM Q experience and QISKit open-source quantum computing software, in *APS March Meeting Abstracts* (APS, New York, 2018), Vol. 2018, pp. L58–003.

[61] F. M. Dekking, C. Kraaikamp, H. P. Lopuhaä, and L. E. Meester, *A Modern Introduction to Probability and Statistics: Understanding Why and How* (Springer, Berlin, 2005), Vol. 488.